Chemistry of the Total Environment 2021, 1(1): 9-19

GLINTPLUS

ISSN: 2805-3419

Original Article

An easy and cheap procedure to immobilize TiO_2 on glass surfaces using TiO_2/SiO_2 nanocomposite: Characterization and performance for the degradation of micropollutants of emerging concern in aqueous solutions

Matheus P. Paschoalino[a], Flávia C. S. Paschoalino[a], Wilson F. Jardim[a], and Fernando F. Sodré[b, *]

[a] Institute of Chemistry, University of Campinas, 13083-970, Campinas, SP, Brazil; [b] Institute of Chemistry, University of Brasília, 70910-000, Brasília, DF, Brazil

ABSTRACT

A simple high area TiO_2/SiO_2 nanocomposite was synthesized, characterized, and used to support P25 TiO_2 on glass surfaces leading to an ease and cheap way to promote adhesion without refined pre-treatment steps. Photocatalytic performance and stability of the immobilized TiO_2 was evaluated in laboratorial and pilot scales, under artificial and solar lights. Degradation rates of 80% and 45% were obtained for salicylic acid (16 mg L^{-1}) and 17β-estradiol (E2, 1.0 mg L^{-1}), respectively, after 4 h using a lab-made annular reactor. Solar batch experiments show a degradation rate of 85% for E2 (10 μg L^{-1}) after 90 min. Photodegradation of trimethoprim (TMP, 500 μg L^{-1}) and levofloxacin (LEVO, 1.0 mg L^{-1}) using a compound parabolic concentrator (CPC) solar reactor revealed removal rates of 50% (once-through experiment) and 95% (batch experiment), respectively. CPC experiments show that the coated composite presents high physical stability after innumerous cycles (more than 2000) under vigorous flow in continuous and batch operation. Overall, results evidenced the efficacy of the TiO_2/SiO_2 composite coated with P25 TiO_2 on the degradation of micropollutants of emerging concern with low energetic costs.

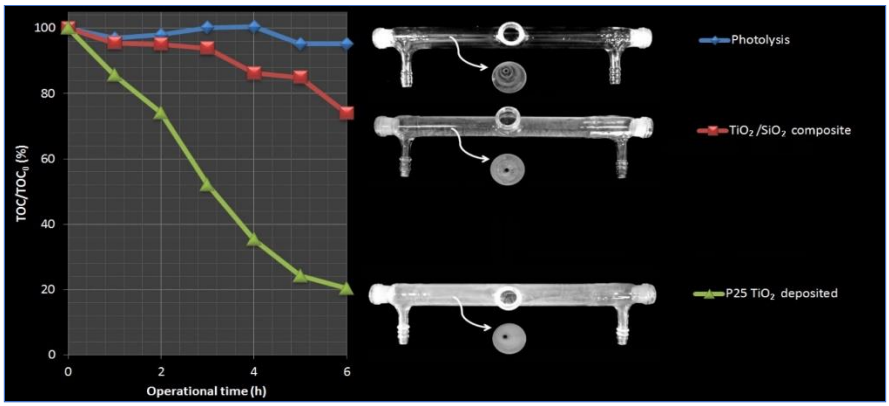

HIGHLIGHTS

- A TiO_2/SiO_2 nanocomposite was synthetized as support for TiO_2 onto glass surfaces.
- The nanocomposite shows good adhesion on glass surfaces after simple coating steps.
- TiO_2 was successfully immobilized in the glass/nanocomposite surface.
- Degradation under artificial light was assessed for salicylic acid and estradiol.
- Solar light provided degradation for estradiol and antimicrobials at ppb levels.

Article History:
Received: 5th January, 2021
Accepted: 9th April, 2021
Available online: 25th May, 2021

Keywords:
Titanium dioxide; silicon dioxide; heterogeneous photocatalysis; compound parabolic concentrator; emerging contaminants.

1. Introduction

A number of advanced oxidation processes (AOP) have been well established in the past few years for the degradation of hazardous chemicals (Chang et al., 2009; Chen et al., 2006; Esplugas et al., 2002; Rosenfeldt & Linden, 2004). The elimination of both gaseous and aqueous organic contaminants is successfully accomplished using AOP based on heterogeneous photocatalysis. These processes are based on the irradiation of a semiconductor with appropriate radiation sufficient to promote electrons from the valence to the conduction band, thus generating oxidative and reductive sites on the catalyst surface (Gaya & Abdullah, 2008; Guillard et al., 1999).

Different semiconductors can be employed in heterogeneous photocatalysis experiments. However, the vast majority of reports shows that Degussa P25 titanium dioxide (TiO_2) presents the most desirable characteristics

* CONTACT: F. F. Sodré; ffsodre@unb.br; Institute of Chemistry, University of Brasília, 70910-000, Brasília, DF, Brazil.
https://doi.org/10.52493/j.cote.2021.1.10

such as adequate surface area (~ 50 m^2 g^{-1}), small particle size (~ 30 nm), a complex microstructure that inhibits electronic recombination, and a crystalline composition (~ 70% anatase and 30% rutile) that promotes high photoactivity with low photocorrosion of the catalyst (Faisal et al., 2007; Fox & Dulay, 1993; Gaya & Abdullah, 2008; Hoffmann et al., 1995; Singh et al., 2007). Also, P25 TiO_2 can be successfully used as a suspension (Dijkstra et al., 2001; Gogate & Pandit, 2004), or in the supported form (Cho et al., 2004; Guillard et al., 2002; Paschoalino et al., 2006). Suspension-based treatments, although efficient, should include an additional step to remove the catalyst from the solution, which can represent a major drawback (Bideau et al., 1995; Farreras & Curcó, 2001). Consequently, the use of supported TiO_2, mainly on glass surfaces, became a desirable alternative in heterogeneous photocatalytic methods.

The most common techniques for supporting a catalyst involve the direct physical deposition of an active solid, such as the P25 TiO_2, or the *in situ* preparation of the catalyst from a precursor by sol-gel methods (Bideau et al., 1995). There are also several ways to support a catalyst on an appropriate surface. Dip coating remains the most used technique for solid and liquid precursors, but other techniques such as spin coating, spray pyrolysis, atomic layer deposition, layer-by-layer self-assembling, ion beam, and DC magnetron sputtering deposition are also used (Mitzi, 2004; Ng et al., 2008; Permpoon et al., 2008; Takeda et al., 2001). Alternatively, catalyst incorporation onto a substrate, usually a polymer, followed by a suitable treatment to expose the catalyst (Paschoalino et al., 2006), or the use of an intermediary material to promote an adequate adhesion of the catalyst on the working surface has already been reported with satisfactory photocatalytic activities (Permpoon et al., 2008).

Considering the increasing interest in support-based methods for heterogeneous photocatalysis, as well as the development of novel strategies for the removal of organic contaminants in aqueous solutions, this paper addresses three objectives. First, to synthesize and characterize a high surface area TiO_2/SiO_2 nanocomposite to be used as a support to for P25 TiO_2 adhesion on glass surfaces. Second, to propose a simplified procedure for the adhesion of TiO_2 without the need for pre-treatment steps. Third, to evaluate the photocatalytic performance of the nanocomposite with and without the TiO_2 adhesion under artificial and solar irradiations.

Four model micropollutants were used in the experiments: salicylic acid (SA), 17β-estradiol (E2), trimethoprim (TMP) and levofloxacin (LEVO). SA is a widely used model because of its analogy to organic moieties on humic structures (Mercê et al., 2006). On the other hand, the degradability of E2 is especially important since it is considered one of the most hazardous micropollutant of emerging concern (Pereira et al., 2015; Sodré & Sampaio, 2020) and presents the highest resistance to direct UV-C photolysis when compared to other endogenous estrogens (Liu & Liu, 2004). The antimicrobial TMP presents a high use pattern in Brazil, where part of this work was carried out (Locatelli et al., 2011), whereas LEVO is a third-generation quinolone commonly used in Europe. Both antimicrobials have been widely investigated in environmental compartments (Locatelli et al., 2011; Tolboom et al., 2019).

2. Materials and methods

2.1 Chemicals and reagents

All chemicals were of high purity or analytical grade. Methanol, ethanol, and propan-2-ol were obtained from Honeywell International (Muskegon, USA) and were used without further chemical purification. Perchloric acid (70%) was purchased from Reagen (Colombo, Brazil). Tetraethylorthosilicate (TEOS) and titanium (IV) isopropoxide were both supplied by Acros Organics (Geel, Belgium). Degussa P25 TiO_2 (Frankfurt on Main, Germany) was used in all photocatalytic experiments. Deionized water was produced in a Milli-Q Plus equipment (Millipore, USA) and reagent water was obtained from J. T. Baker (Xalostoc, Mexico).

E2, SA, TMP and LEVO standards were purchased from Sigma-Aldrich (St. Louis, USA). Chemical structures of the compounds are presented in Figure 1. Working solutions (16 mg L^{-1} SA, 1.0 mg L^{-1} and 10 µg L^{-1} E2; 500 µg L^{-1} TMP and 1.0 mg L^{-1} LEVO) were prepared using commercial bottled water.

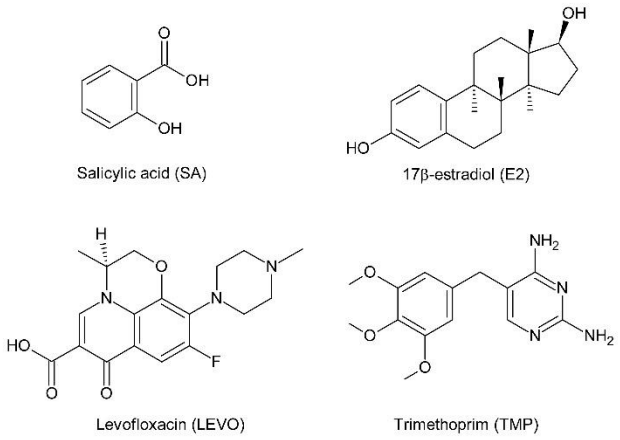

Figure 1: Chemical structures of the investigated micropollutants of emerging concern.

2.2. Photocatalytic devices

Experiments using artificial light were performed in a small lab-made annular photocatalytic reactor, as shown in Figure 2, consisting of a 280 mm long glass cylindrical tube (inner diameter of 22 mm) surrounding a 300 mm long compact fluorescent lamp (outer diameter of 15 mm) as the central annulus. An UV black light fluorescent lamp (Ecolume ZG 8 W, λ_{max} = 365 nm, 2.39 mW cm^{-2}) was employed in all experiments with a net volume of 50 mL and 154.6 cm^2 of exposed catalyst area.

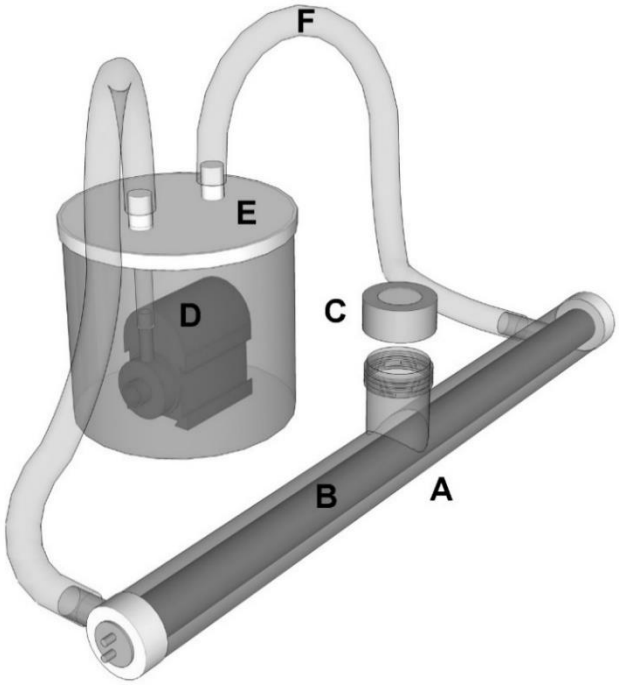

Figure 2. The lab-made photocatalytic reactor used in the experiments carried out using artificial light: (A) annular lab-made glass reactor, (B) UV black light fluorescent lamp, (C) silicon septum in the sampling device, (D) recirculation pump, (E) reservoir, (F) silicone connecting tubes.

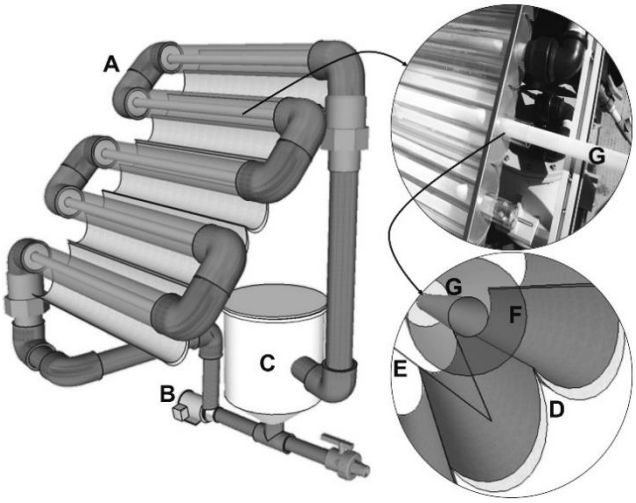

Figure 3. Scheme of the solar reactor used: (A) CPC; (B) recirculation pump; (C) 35 L polypropylene reservoir; (D) detail of W-shape foil mirror collector; (E) representation of UV radiation collected; (F) borosilicate glass pipe; (G) TiO_2 P25 deposited onto cylindrical glass precoated with the TiO_2/SiO_2 nanocomposite.

A vial section with a screw cap silicone septum was used as a sampling device. Two tubular glass sections were placed at the ends of the photoreactor to allow the circulation of the working solutions, provided by a submerged pump (Vigo Ar A300) placed inside a 500 mL reservoir flask. All the connecting tubes used in the reactor system were made of silicone.

Preliminary solar photocatalytic experiments were carried out in glass Petri dishes (internal diameter of 5.1 cm and total area of 20.4 cm^2). Pilot solar experiments were carried out using a reactor (Figure 3) equipped with a compound parabolic concentrator (CPC) (AoSol, Portugal) containing five W-shape coaxial-type solar collectors manufactured with aluminum foil mirrors totalizing a surface collector area of 1 m^2. These structures collect and focus both direct and diffuse solar radiation onto transparent borosilicate glass pipes (1500 mm long, 50 mm o.d., Schott, Germany) enclosing coaxial cylindrical glass pieces (1500 mm x 32 mm) which were coated with the TiO_2/SiO_2 composite totalizing 0.71 m^2 area with a net volume of 0,29 L. The system also comprises a 12 W centrifugal pump (Figure 3(b); NH-10PX-H, Pan World, Japan), a rubber sampling port and a 35 L polypropylene reservoir (Roca i Roca, Barcelona, Spain) with a venting filter.

2.3. Synthesis of the TiO_2/SiO_2 nanocomposite

A conventional sol-gel synthesis was carried out for the preparation of the TiO_2/SiO_2 nanocomposite. Two solutions, named A and B, were used. Solution A was a mixture of 1.1 mL of titanium(IV)isopropoxide and 23 mL of propan-2-ol. Solution B was prepared by adding 2.8 mL of perchloric acid and 1 mL of TEOS in deionized water (1 L). An appropriate flask containing solution B was kept in an ice bath under continuous stirring. Then, solution A was gradually added to the flask to form the nanocomposite support. After several experiments, optimal synthesis conditions were selected as follows: stirring time of 48 h, drying step at 60 °C for 24 h and calcination at 800 °C for 8 h after heating at a rate of 50 °C min^{-1}. The calcinated TiO_2/SiO_2 was crushed to powder, washed several times using deionized water and dried again at 60 °C for 24 h.

2.4. TiO_2/SiO_2 support characterization

The diffuse reflectance spectrum of the TiO_2/SiO_2 nanocomposite was recorded in the UV-Visible region employing a Varian Cary 5G spectrophotometer. The nanocomposite was also characterized by Fourier transform infrared spectroscopy (FTIR) using a Perkin Elmer Espectrun ONE analyzer from 4000 to 400 cm^{-1}. Phase composition and crystallite size determinations were obtained by X-ray diffractometry (XRD) using a Shimadzu XRD7000 diffractometer with Cu-Kα radiation. Surface analysis was also evaluated by scanning electron microscopy (SEM) using a JEOL JSM-6360 LV instrument operated at 20 kV and coupled to a NORAN System SIX energy dispersive X-ray spectrometer (EDX). Nitrogen physisorption isotherms were measured on a Micrometrics ASAP 2010 analyzer at 77.3 K. The specific surface area of the nanocomposite was calculated using the Brunauer-Emmett-Teller (BET) method.

2.5. Coating procedures on glass surfaces

For all tests coating was performed in two steps: Firstly, 10 mL of a 7.0 mg mL^{-1} TiO_2/SiO_2 suspension prepared in a 1:1 ethanol:water mixture (v/v) was maintained in contact with the glass surfaces under vigorous stirring for 5 min, and dried at 60 °C for 5 min. Repetitive coating steps were performed up to five times to enhance the TiO_2/SiO_2 layer thickness. After this preliminary treatment, P25 TiO_2 was deposited onto the previously TiO_2/SiO_2-coated surfaces in the same manner as described above. However, in this case, a 10 mg mL^{-1} suspension was prepared in a 1:1 ethanol:water mixture (v/v). Again, up to five P25 TiO_2 coating steps were performed. Between each step, the surfaces were thoroughly washed with deionized water to remove loose particles. Figure 4 shows the visual aspect of the lab-made reactor at different steps of the catalyst deposition onto the glass surface.

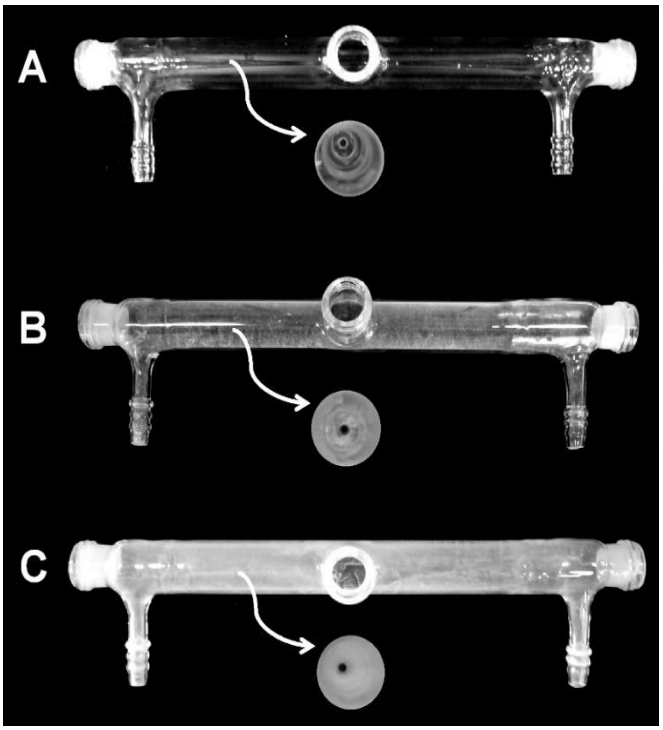

Figure 4. External and internal views of the glass cylindrical tube used in the lab-made reactor: (A) untreated glass surface, (B) glass surface after TiO_2/SiO_2 nanocomposite coating and (C) glass surface after P25 TiO_2 deposition over the TiO_2/SiO_2 layer.

2.6. Photodegradation of SA and E2

The photodegradation of SA (16 mg L^{-1}) and E2 (1 mg L^{-1}) was evaluated under artificial light in batch experiments using a recirculation flow rate of 20 L h^{-1}. E2 photodegradation was also evaluated using solar radiation by placing ten milliliters of the test solution (0.01 mg L^{-1}) into Petri dishes and irradiated for 3 h by natural solar radiation (average of 3.15 mW cm^2 measured with a 9811 Cole Parmer radiometer at λ = 365 nm) in good weather conditions during summer in the University of Campinas (São Paulo, Brazil). For all experiments, zero reaction time was counted immediately after the lamp was turned on or after sunlight exposition.

SA degradation was monitored by total organic carbon determinations using a TOC analyzer (Shimadzu TOCV-CPN) and by UV-Vis absorbance using a Jenway 6405 spectrophotometer. E2 concentration was monitored by mass spectrometry using an Agilent 1200 Series LC system coupled to an Agilent 6410 TripleQuad mass spectrometer (Palo Alto, USA). During the experiments, E2 aliquots were taken, filtered on PTFE filters (0.2 µm porosity), and directly injected without further extraction procedures using a Zorbax SB-C18 column (2.1 x 30 mm, particle size of 3.5 µm, Agilent Technologies) with 10:90 water:methanol isocratic elution at a flow rate of 0.3 mL min^{-1}. Ionization was performed using an electrospray interface operating in the negative ion mode. E2 quantification was achieved using multiple reaction monitoring parameters optimized elsewhere (Sodré et al., 2010).

2.7. Photodegradation of TMP and LEVO using the CPC solar reactor

The photoreactor was positioned tilted 40º and aligned in an east-west direction on top of the Chemistry building on the Complutense University of Madrid (Spain) at 40 ºN in good weather conditions during the most intense UV radiation period for Madrid. UV intensity data were provided by Spain's meteorological agency (AEMET).

Two trials were carried out using the CPC solar reactor: (a) continuous photodegradation (once-through experiment) of 30 L TMP solution (500 µg L^{-1}) pumped at 0.2 L min^{-1} flow rate during 70 min and (b) batch photodegradation of 20 L LEVO solution (1 mg L^{-1}) at 2 L min^{-1} recirculation rate during 300 min. For all experiments, zero reaction time was counted immediately after CPC exposition to sunlight.

Before tests, the reactor was kept protected from sunlight for 30 min to permit system stabilization. Three control experiments were carried out during all trials, one in the dark, to assess the adsorption of the analytes on the glass surface, and the other two, with and without direct physical deposition of P25 TiO2 on glass, in order to investigate the efficiency of the nanocomposite and the effect of direct photolysis, respectively. Aliquots were taken at pre-determined times, filtered on PTFE filters (0.2 µm porosity) and directly injected without further extraction procedures in an Agilent 1100 Series LC system using an Aqua C18 (250 mm × 4.6 mm ID, 5 µm) column. An isocratic elution was performed using mobile phase of 26:74 acetonitrile:water (0.5% acidified with trifluoracetic acid) in a flow rate gradient from 0.5 to 1.0 mL min^{-1}. TMP was detected using DAD at 230 nm and LEVO was detected using FLD (λ_{ex} = 280 nm; λ_{em} = 515 nm).

3. Results and discussion

3.1. Characterization of the support

After testing several synthetic routes (varying TEOS volume and calcination temperatures) the proportions of reactants as described in the experimental section provided a solid TiO_2/SiO_2 material with a BET surface area of 315 m^2 g^{-1}. Reports in the literature indicate that solids with high surface areas, such as the one synthesized in this work, are suitable to use as supports in photocatalysis (Garcia-Rodríguez et al., 2014; Rusu & Yates, 2001). A high surface area leads to an increase on the photocatalyst aggregation in the working surface, probably enhancing the efficiency of photocatalytic systems (Li et al., 2007; Mikula et al., 1995). The pores of the synthesized TiO_2/SiO_2 support were generally mesoporous (Everett, 1972), with an average pore diameter of about 5 to 6 nm and a single point pore volume of 0.4595 cm^3 g^{-1}. Additional pore characteristics of the P25 TiO_2 were obtained: BET surface area of 52 m^2 g^{-1}, pore volume of 0.2336 cm^3 g^{-1}, and an average pore diameter of 19 nm. Higher values obtained for the TiO_2/SiO_2 support in comparison to the P25 TiO_2 alone reveals that the proposed synthesis procedure was successful in providing a solid with desirable physiochemical properties.

Figure 5 shows XRD spectra assigned for the P25 TiO_2 photocatalyst and for the TiO_2/SiO_2 support after different calcinations steps. Despite the high temperature (800 °C) and the long time (8 h) employed in the calcination process, XRD spectra (Figure 5(b)) reveal that anatase phase (2θ = 25°) was stabilized with the addition of TEOS avoiding the well-known complete conversion of anatase to rutile (2θ = 27°) at temperatures above 500 °C. A characteristic weak and broad diffraction around 2θ = 25° (Figures 5(a) and (b)) indicates that silica was mostly in the amorphous form in the TiO_2/SiO_2 nanocomposite with little interference on TiO_2 crystallinity (Mikula et al., 1995).

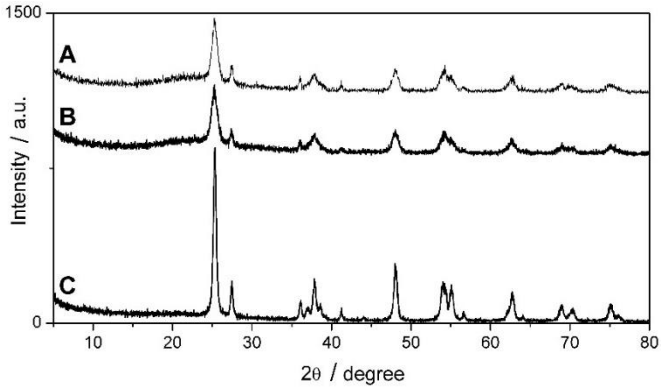

Figure 5. XRD patterns of the solids used in this work: (A) two-step calcination of the TiO_2/SiO_2 nanocomposite, (B) one-step calcination of the TiO_2/SiO_2 nanocomposite and (C) P25 TiO_2 photocatalyst.

Anatase percentage in the TiO_2/SiO_2 nanocomposite was calculated using equation (1) where f is the weight fraction of anatase in the sample, while I_A and I_R are the intensities of the strongest anatase and rutile peaks in the XRD spectrum, respectively (Xu et al., 2003). The ratio between anatase and rutile phases in TiO_2-based solids is related to the increase of the TiO_2 (photo)chemical stability since rutile is the thermodynamically stable phase while anatase is the most photoactive phase. Considering the data in Figure 5(a) and (b), an anatase percentage of 49% was estimated for the TiO_2/SiO_2 nanocomposite, indicating that the solid could be less photoactive than P25 (Figure 5(c)) that presents an anatase percentage of 77%.

$$f = \left(1 + 1.26 \frac{I_R}{I_A}\right)^{-1} \quad (1)$$

Crystal sizes of the TiO_2 in the final nanocomposite were estimated using the most intense (101) peak (2θ = 25°) with its full line width at half of the maximum peak intensity from the Debye–Scherrer formula (equation 2) reported elsewhere (Keshmiri et al., 2004; Trung & Ha, 2004).

$$L = \frac{k\,\lambda}{\beta \cos\theta} \quad (2)$$

In equation 2, L represents the average crystal size (nm); k is a constant equal to 0.90, λ is the XRD radiation wavelength (1.5418 nm); β indicates the excess line broadening (radians) and θ is the Bragg angle (radians). The crystallite size of the TiO_2 on the TiO_2/SiO_2 nanocomposite was 27 nm while the P25 TiO_2 presented a value of 31 nm.

A two-step calcination procedure was also performed and showed no relevant alterations in the synthesized solid as shown in the XRD spectra (Figure 5(a)). However, a decrease in the BET surface area to 137 m^2 g^{-1} was noticed for the two-step calcinated nanocomposite, limiting its use as a support at high temperatures. Because of this, after synthesis, this solid was deposited on glass using a maximum temperature of 60 °C.

Figure 6 shows UV-Vis reflectance and FT-IR spectra for the solid materials used in this work. Reflectance data in Figure 6(a) reveal small alterations in the band-gap of TiO_2, which confirms that the spectrum, in grey line, is exclusively formed as a consequence of TiO_2, as previously reported in the literature (Aguado et al., 2006).

As shown in Figure 6(b), both spectra present the well know vibrations for Ti-O stretching (around 470 cm^{-1}), and the TiO_2/SiO_2 spectrum (black line) also shows a Si-O-Si asymmetric stretching around 1070 cm^{-1}. These results corroborate the TiO_2 co-precipitation with silica, as suggested by the XRD data, since no relevant peak around 950 cm^{-1}, relative to the Ti-O-Si bonds, was noticed (Xu et al., 2003; Yu & Wang, 2000). Bands in the region around 3450 to 3400 cm^{-1} are assigned to the characteristic bending vibrations of adsorbed water molecules. Finally, the shape of the TiO_2/SiO_2 spectrum is typical for composites with a

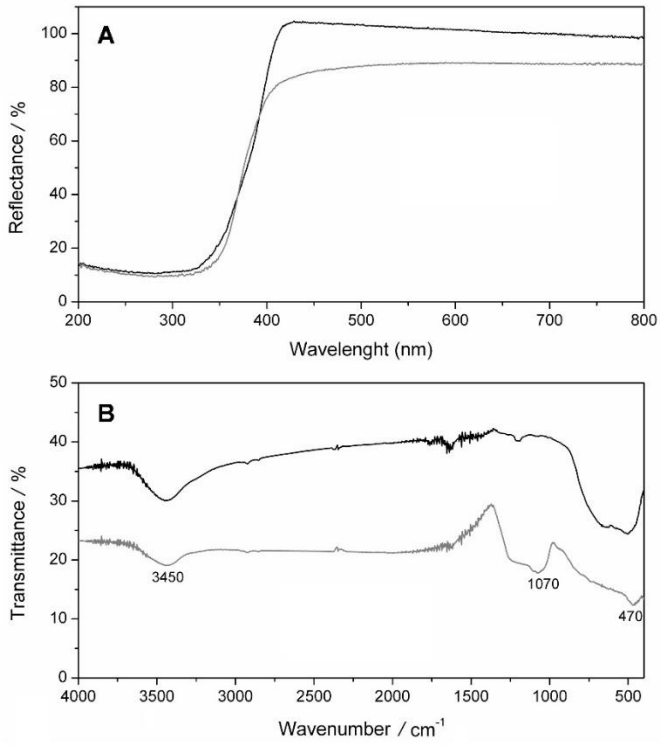

Figure 6. Reflectance (A) and FT-IR (B) spectra of the P25 TiO_2 photocatalyst (black line) and the TiO_2/SiO_2 nanocomposite (grey line).

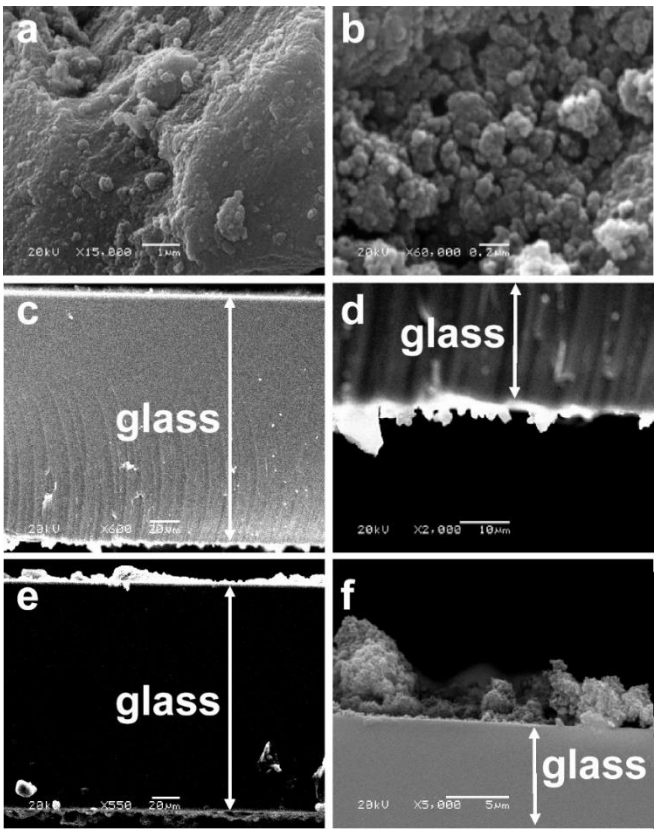

Figure 7. SEM micrographs of TiO_2/SiO_2 nanocomposite. (A) Powder form with a X15,000 magnification, (B) Powder form with a X60,000 magnification, (C) TiO_2/SiO_2 deposited in both sides of a glass coverslip with a X600 magnification, (D) TiO_2/SiO_2 deposited in both sides of a glass coverslip with a X2,000 magnification, (E) P25 TiO_2 deposited over the TiO_2/SiO_2 with a X550 magnification, and (F) P25 TiO_2 deposited over the TiO_2/SiO_2 with a X5,000 magnification.

50:50 Ti/Si atomic ratio, as previously confirmed using EDX data (Murashkevich et al., 2008).

Figure 7 presents the SEM micrographs of the TiO_2/SiO_2 nanocomposite in the powder form as well as at different deposition stages in the working surfaces. It is possible to observe in Figures 7(a) and (b), relative to the powdered TiO_2/SiO_2 nanocomposite, typical agglomeration patterns attributed to TiO_2. In this case, highly porous particles (50 to 500 nm) are deposited on bigger particles (30 to 50 μm). Considering that the TiO_2/SiO_2 nanocomposite deposition was carried out using the synthesized solid in the powder form, an irregular layer was noticed instead of a well-defined film formed during traditional homogeneous sol-gel based methods. Figures 7(c) and (d) show lateral fracture micrographs of the TiO_2/SiO_2 nanocomposite deposited on both sides of the glass surface, where a layer varying from 0.5 to 15 μm was determined. Finally, this irregular surface contributed to a satisfactory P25 TiO_2 adhesion over the deposited support as illustrated in Figures 7(e) and (f).

EDX spectra of the deposited solids are presented in Figure 8 at different regions (named a, b, and c) of the fractured glass coverslip. Region (c) spectrum, which corresponds to the middle of the glass coverslip, shows an intense peak attributed to Si, as expected. On the interface region (b), a confirmation peak attributed to Ti appears in the spectrum as an indication of the presence of TiO_2, probably from the TiO_2/SiO_2 support. Finally, at the external region (a) two well defined Ti peaks between 4 and 5 keV show the effective deposition of P25 TiO_2 over the TiO_2/SiO_2 support.

3.2 Photocatalytic experiments

During the photocatalytic tests with TiO_2/SiO_2 support, a high reuse capability was observed even when high flow rates were used, when compared with P25 directly deposited on glass, which leaches with the solution flow rate. Probably weak van de Waals intermolecular forces between the glass and the nanocomposite promoted good adhesion as a result of the deposition procedure employed (Howe et al., 1955). The support only could be removed by mechanical abrasion.

Figures 9 and 10 show the photocatalytic support performance for SA and E2 degradation, respectively. After six hours of irradiation, the classical model-compound SA was 80% mineralized when using P25/TiO_2/SiO_2 supported on the reactor walls, promoting total SA degradation after four hours, as confirmed by the UV spectrum (Figure 9(c)). When the TiO_2/SiO_2 was deposited alone (without P25), a mineralization of 25% was achieved with a concomitant decrease in the UV absorption bands, but without significant spectral alterations (Figure 9(b)). Photolysis was not

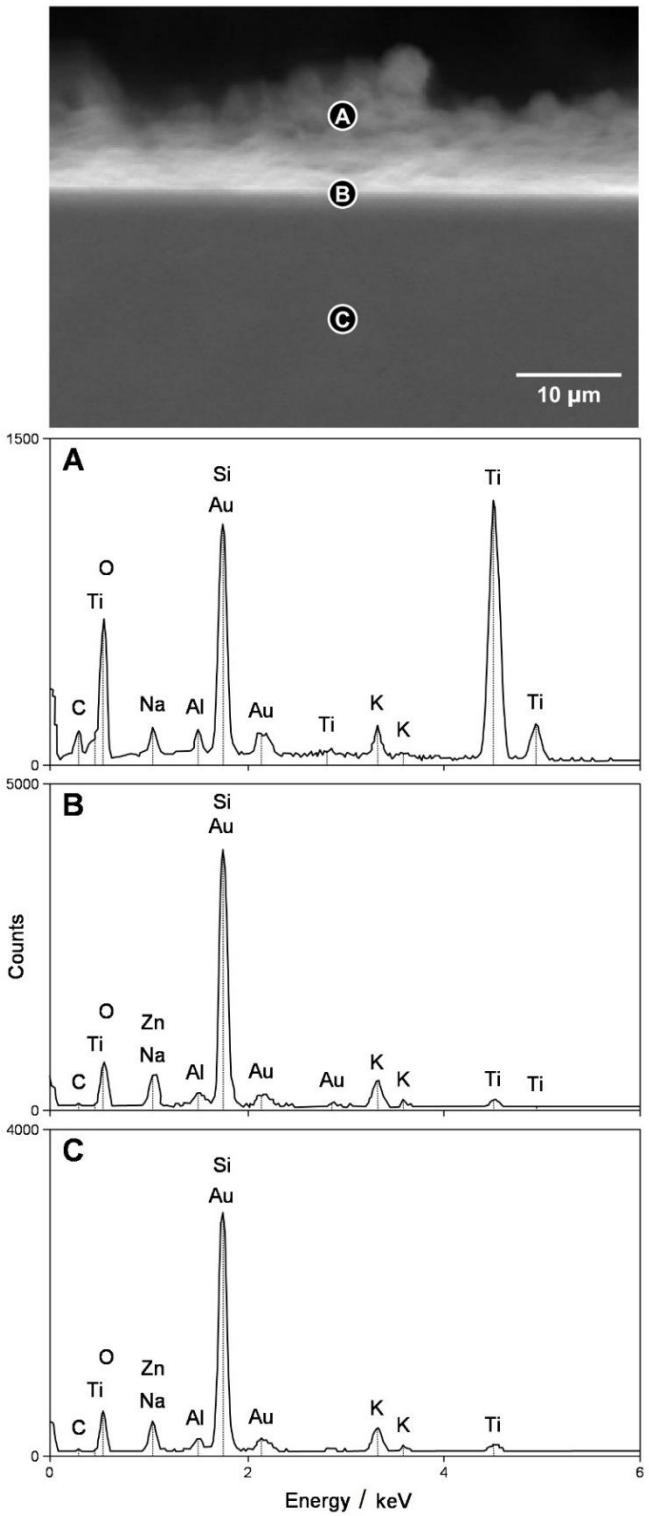

Figure 8. EDX spectra for three different regions of the solids deposited on the glass surface: (A) external surface related to the deposited P25 TiO_2, (B) glass/support interface related to deposited TiO_2/SiO_2 and (C) glass coverslip substrate.

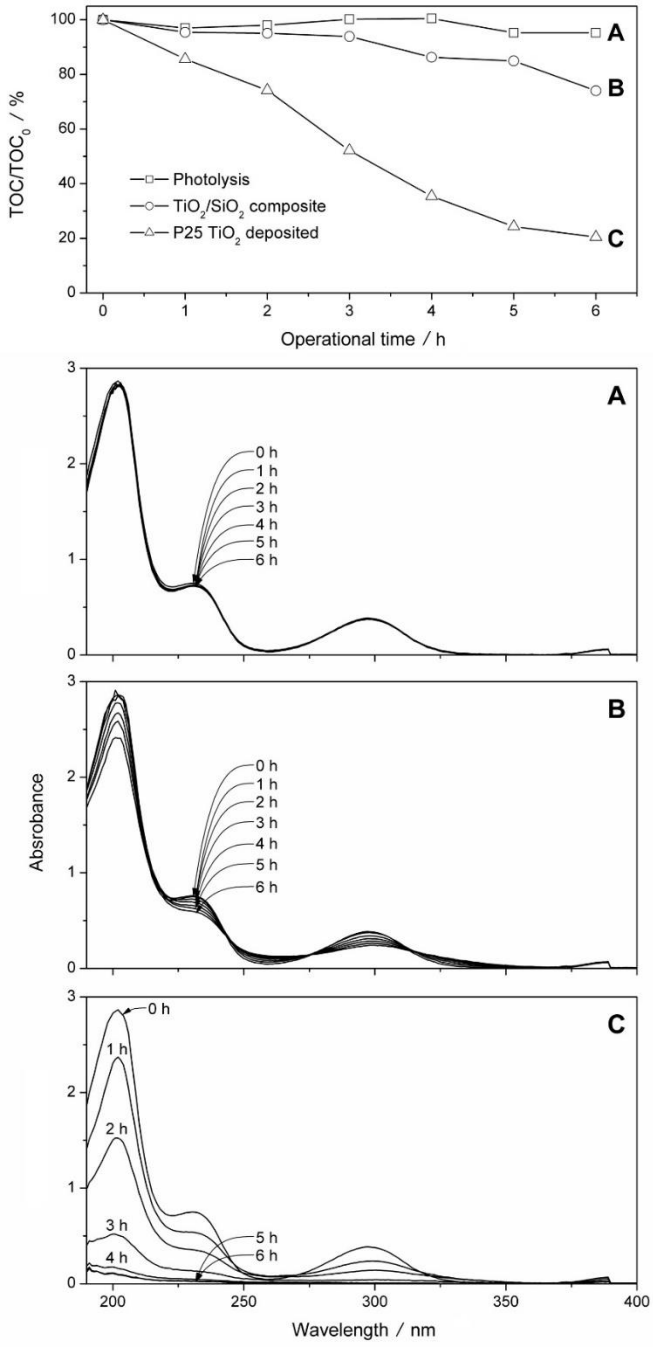

Figure 9. SA (16 mg L^{-1}) degradation in a lab-made reactor (300 mL) monitored by TOC and UV absorption promoted by: (A) photolysis (BLB lamp, 8 W, λ ~ 365 nm), (B) TiO_2/SiO_2 nanocomposite and (C) P25 TiO_2 deposited over TiO_2/SiO_2.

significant (less than 10% mineralization) without changes in the UV spectrum (Figure 9(a)).

Figure 10 shows E2 degradation under two different conditions. When the lab-made reactor was employed, almost 60% degradation of a 1 mg L^{-1} solution was achieved after an 8 h operation, as illustrated in Figure 10(a). Under solar light, a degradation of 85% was achieved after 90 min of exposure, but in a Petri dish filled with a 0.01 mg L^{-1} solution, without stirring and with a volume 30 times lower than that shown in Figure 10(a). Photolysis was responsible for 20% degradation in the 10A case and for 10% for the condition used in 10B at the end of both experiments. It is worth mentioning that the difference in the irradiation time

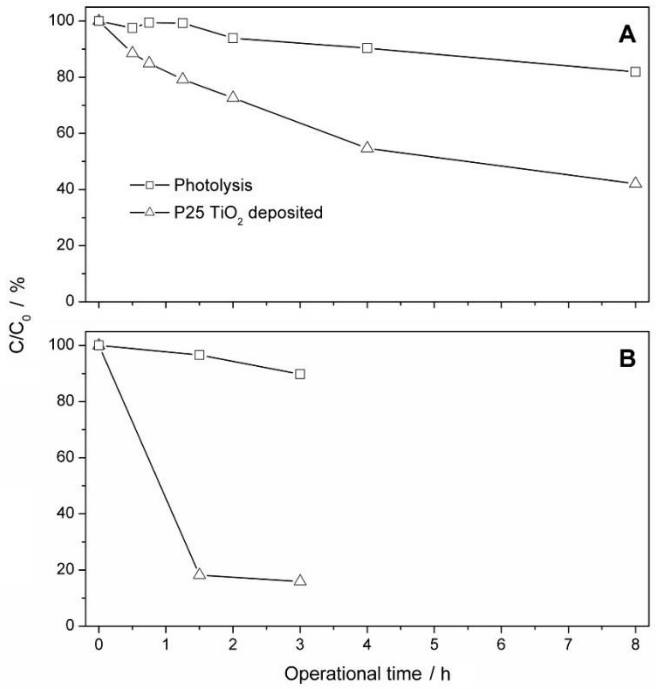

Figure 10. E2 degradation (A) 1 mg L^{-1} promoted by 300 mL lab-made reactor (BLB lamp, 8 W, λ ~365 nm) and (B) 0.01 mg L^{-1} promoted by solar light on Petri plates (10 mL).

is due to the fact that solar experiments were set to explore the maximum radiation period (11-14 h). Control experiments, carried out in the dark, presented adsorption around 5% for the test solutions. No results were obtained for the control experiment carried out with the direct physical deposition of the catalyst due to its leaching.

Preliminary results obtained were satisfactory when compared to data from other studies, as reported by Ohko et al. (2002) who showed degradation rates higher than 99 % for a 0.27 mg L^{-1} E2 solution (50 mL) after 30 min UV irradiation using a 1.0 g L^{-1} P25 suspension and a UV intensity 3 times higher than the one employed in the present work. Zhang et al. (2007) achieved complete E2 (0.1-1.0 mg L^{-1}) degradation with similar times (1-4 h), also employing a 1 g L^{-1} P25 suspension in a large reactor (700 mL) equipped with a powerful lamp (150 W). Coleman et al. (2000) used P25 supported over a 1 cm^2 Ti-Al-V alloy to achieve a degradation rate of 96% of an 8-mL E2 solution (~0.02-1.0 mg L^{-1}), after 3.5 h and with a UV intensity 5.5 times higher. Considering the electricity consumption to degrade 1 g of E2, the lab-made reactor used in this work was effective consuming 355 kW.h, a value considered low when compared to 7407 kW.h, 1500 kW.h and 65625 kW.h obtained elsewhere for this same compound (Coleman et al., 2000; Ohko et al., 2002; Zhang et al., 2007).

In the final trials, using the solar CPC reactor, it was possible to test the resistance to the flow of water in a bigger scale experiment. In the first assay, TMP solution was submitted to an once-through experiment achieving an average degradation of 30% after the reactor residence time (~30 min). This value could reach 50% after 70 min in some experiments as showed in Figure 11.

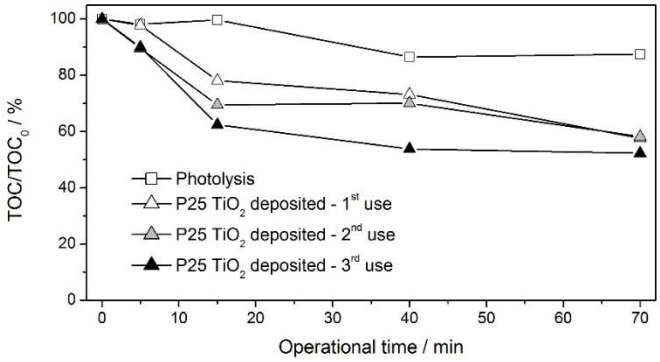

Figure 11. Remaining percentage of TMP (500 μg L^{-1}) on the reuse of P25 TiO_2 surface in a once-through experiment (0.2 L min^{-1}) experiment toward the CPC solar reactor.

The high variation observed in Figure 11 is mainly due to the different UV solar radiation in each experiment. In addition, considering the CPC reactor net volume of 0.29 L, the flow rate (0.2 L min^{-1}) and the total time spent after three consecutive uses (210 min), no signal of the P25 TiO_2 surface deactivation was observed after 145 cycles, where each cycle refers to the complete filling of the reactor's net volume. Considering that these trials were carried out in single pass using a TMP concentration similar to that found in surface water or sewage (Nikolaou et al., 2007) the system could be considered efficient, since photolysis was responsible to only 10% degradation and the dark adsorption process was not significant.

In the second trial, LEVO photodegradation was investigated under batch conditions during 300 min. To normalize the trial conditions, the UV accumulated dose during each experiment was used.

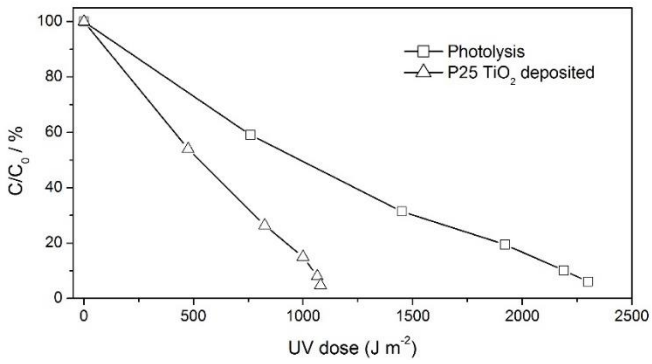

Figure 12. Normalized remaining concentration of LEVO (20 L, 1 mg L^{-1}) under photolysis and photocatalysis process using the CPC solar reactor operating in batch mode at 2 L min^{-1} recirculation rate.

In Figure 12 it is possible to observe that the photocatalytic process was again very efficient since a larger dose of UV would be needed to degrade the same amount of LEVO solely by photolysis (2300 J m^{-2} against 1100 J m^{-2}). Adsorption processes were insignificant (less than 1% removal). Considering the CPC reactor net volume, a higher

flow rate (2 L min^{-1}) in comparison with the TMP experiment and a total time of 300 min, no signal of the catalyst surface deactivation was observed after more than 2000 cycles.

4. Conclusion

The TiO_2/SiO_2 nanocomposite synthesized showed good physicochemical properties as support for photocatalytic purposes, mainly due to its high surface area, which was comparable to commercial SiO_2 beads (Nishikawa & Takahara, 2001), associated with its good adhesion onto glass surfaces without further treatment steps. Solar experiments using a CPC reactor revealed that the coated nanocomposite presented high physical stability after innumerous reuse cycles under vigorous flow, achieving an average of 50% of TMP degradation in continuous operation (once-through experiment) and 95% for LEVO in batch operation. Results showed that is necessary a UV dose twice higher to obtain the same degradation rate by photolysis. Solar tests also showed that the support developed could be a good surface to be used in the construction of simple solar photocatalytic systems to destroy emerging compounds such hormones and antibiotics with high efficiency and low energy costs.

CRediT authorship contribution statement

MPP: Methodology, Writing - original draft, Writing - review & editing. FCSP: Methodology. WFJ: Conceptualization, Supervision. FFS: Methodology, Writing - original draft, Writing - review & editing Data curation, Software.

Declaration of competing interest

The authors declare that they have no known competing financial interests or personal relationships that could have appeared to influence the work reported in this paper.

Acknowledgement

The authors acknowledge CNPq and FAPESP for their financial support. They also thank Prof. Guillermo Orellana and Prof. Maria Cruz Moreno-Bondi from Universidad Complutense de Madrid for technical support during solar degradation experiments and Prof. Carol H. Collins for revising the manuscript.

References

Aguado, J., van Grieken, R., López-Muñoz, M.-J., & Marugán, J. (2006). A comprehensive study of the synthesis, characterization and activity of TiO_2 and mixed TiO_2/SiO_2 photocatalysts. *Applied Catalysis A: General*, *312*, 202–212. https://doi.org/10.1016/j.apcata.2006.07.003

Bideau, M., Claudel, B., Dubien, C., Faure, L., & Kazouan, H. (1995). On the "immobilization" of titanium dioxide in the photocatalytic oxidation of spent waters. *Journal of Photochemistry and Photobiology A: Chemistry*, *91*(2), 137–144. https://doi.org/10.1016/1010-6030(95)04098-Z

Chang, H.-S., Choo, K.-H., Lee, B., & Choi, S.-J. (2009). The methods of identification, analysis, and removal of endocrine disrupting compounds (EDCs) in water. *Journal of Hazardous Materials*, *172*(1), 1–12. https://doi.org/10.1016/j.jhazmat.2009.06.135

Chen, W. R., Sharpless, C. M., Linden, K. G., & Suffet, I. H. (2006). Treatment of volatile organic chemicals on the EPA Contaminant Candidate List using ozonation and the O_3/H_2O_2 advanced oxidation process. *Environmental Science & Technology*, *40*(8), 2734–2739. https://doi.org/10.1021/es051961m

Cho, M., Chung, H., Choi, W., & Yoon, J. (2004). Linear correlation between inactivation of *E. coli* and OH radical concentration in TiO_2 photocatalytic disinfection. *Water Research*, *38*(4), 1069–1077. https://doi.org/10.1016/j.watres.2003.10.029

Coleman, H. M., Eggins, B. R., Byrne, J. A., Palmer, F. L., & King, E. (2000). Photocatalytic degradation of 17-β-oestradiol on immobilised TiO_2. *Applied Catalysis B: Environmental*, *24*(1), L1–L5. https://doi.org/10.1016/S0926-3373(99)00091-0

Dijkstra, M. F. J., Michorius, A., Buwalda, H., Panneman, H. J., Winkelman, J. G. M., & Beenackers, A. A. C. . (2001). Comparison of the efficiency of immobilized and suspended systems in photocatalytic degradation. *Catalysis Today*, *66*(2), 487–494. https://doi.org/10.1016/S0920-5861(01)00257-7

Esplugas, S., Giménez, J., Contreras, S., Pascual, E., & Rodŕiguez, M. (2002). Comparison of different advanced oxidation processes for phenol degradation. *Water Research*, *36*(4), 1034–1042. https://doi.org/10.1016/S0043-1354(01)00301-3

Everett, D. H. (1972). Manual of symbols and terminology for physicochemical quantities and units, Appendix II: definitions, terminology and symbols in colloid and surface chemistry. *Pure and Applied Chemistry*, *31*(4), 577–638. https://doi.org/10.1351/pac197231040577

Faisal, M., Abu Tariq, M., & Muneer, M. (2007). Photocatalysed degradation of two selected dyes in UV-irradiated aqueous suspensions of titania. *Dyes and Pigments*, *72*(2), 233–239. https://doi.org/10.1016/j.dyepig.2005.08.020

Farreras, J. G., & Curcó, D. (2001). Modelos cinéticos y de radiación en sistemas fotocatalíticos. In M. A. Blesa (Ed.), *Eliminación de contaminantes por fotocatálisis heterogênea* (pp. 189–199). Red CYTED VIII-G.

Fox, M. A., & Dulay, M. T. (1993). Heterogeneous photocatalysis. *Chemical Reviews*, *93*(1), 341–357. https://doi.org/10.1021/cr00017a016

Garcia-Rodríguez, A., Sagristà, E., Matamoros, V., Fontàs, C., Hidalgo, M., & Salvadó, V. (2014). Determination of pharmaceutical compounds in sewage sludge using a standard addition method approach. *International Journal of Environmental Analytical Chemistry*, *94*(12),

1199–1209. https://doi.org/10.1080/03067319.2014.921292

Gaya, U. I., & Abdullah, A. H. (2008). Heterogeneous photocatalytic degradation of organic contaminants over titanium dioxide: A review of fundamentals, progress and problems. *Journal of Photochemistry and Photobiology C: Photochemistry Reviews*, *9*(1), 1–12. https://doi.org/10.1016/j.jphotochemrev.2007.12.003

Gogate, P. R., & Pandit, A. B. (2004). A review of imperative technologies for wastewater treatment I: oxidation technologies at ambient conditions. *Advances in Environmental Research*, *8*(3), 501–551. https://doi.org/10.1016/S1093-0191(03)00032-7

Guillard, C., Beaugiraud, B., Dutriez, C., Herrmann, J.-M., Jaffrezic, H., Jaffrezic-Renault, N., & Lacroix, M. (2002). Physicochemical properties and photocatalytic activities of TiO_2-films prepared by sol–gel methods. *Applied Catalysis B: Environmental*, *39*(4), 331–342. https://doi.org/10.1016/S0926-3373(02)00120-0

Guillard, C., Disdier, J., Herrmann, J.-M., Lehaut, C., Chopin, T., Malato, S., & Blanco, J. (1999). Comparison of various titania samples of industrial origin in the solar photocatalytic detoxification of water containing 4-chlorophenol. *Catalysis Today*, *54*(2), 217–228. https://doi.org/10.1016/S0920-5861(99)00184-4

Hoffmann, M. R., Martin, S. T., Choi, W., & Bahnemann, D. W. (1995). Environmental applications of semiconductor photocatalysis. *Chemical Reviews*, *95*(1), 69–96. https://doi.org/10.1021/cr00033a004

Howe, P. G., Benton, D. P., & Puddington, I. E. (1955). London-Van der Waals attractive forces between glass surfaces. *Canadian Journal of Chemistry*, *33*(9), 1375–1383. https://doi.org/10.1139/v55-165

Keshmiri, M., Mohseni, M., & Troczynski, T. (2004). Development of novel $_{TiO2}$ sol–gel-derived composite and its photocatalytic activities for trichloroethylene oxidation. *Applied Catalysis B: Environmental*, *53*(4), 209–219. https://doi.org/10.1016/j.apcatb.2004.05.016

Li, S., Liu, J., & Feng, T. (2007). Low temperature coating of anatase thin films on silica glass fibers by liquid phase deposition. *Journal of Wuhan University of Technology-Mater. Sci. Ed.*, *22*(1), 136–139. https://doi.org/10.1007/s11595-005-1136-9

Liu, B., & Liu, X. (2004). Direct photolysis of estrogens in aqueous solutions. *Science of The Total Environment*, *320*(2), 269–274. https://doi.org/10.1016/j.scitotenv.2003.08.005

Locatelli, M. A. F., Sodré, F. F., & Jardim, W. F. (2011). Determination of antibiotics in Brazilian surface waters using liquid chromatography-electrospray tandem mass spectrometry. *Archives of Environmental Contamination and Toxicology*, *60*(3), 385–393. https://doi.org/10.1007/s00244-010-9550-1

Mercê, A. L. R., Lopes, P. P., Mangrich, A. S., & Levy, N. M. (2006). Molybdenum (VI) binded to humic and nitrohumic acid models in aqueous solutions. Salicylic, 3-nitrosalicylic, 5-nitrosalicylic and 3,5 dinitrosalicylic acids: part 2. *Journal of the Brazilian Chemical Society*, *17*, 482–490. https://doi.org/10.1590/S0103-50532006000300008

Mikula, M., Brezová, V., Cěppan, M., Pach, L., & Karpinský, Ĺ. (1995). Comparison of photocatalytic activity of sol-gel TiO_2 and P25 TiO_2 particles supported on commercial fibreglass fabric. *Journal of Materials Science Letters*, *14*(9), 615–616. https://doi.org/10.1007/BF00586156

Mitzi, D. B. (2004). Solution-processed inorganic semiconductors. *Journal of Materials Chemistry*, *14*(15), 2355–2365. https://doi.org/10.1039/B403482A

Murashkevich, A. N., Lavitskaya, A. S., Barannikova, T. I., & Zharskii, I. M. (2008). Infrared absorption spectra and structure of TiO_2-SiO_2 composites. *Journal of Applied Spectroscopy*, *75*(5), 730. https://doi.org/10.1007/s10812-008-9097-3

Ng, C. J. W., Gao, H., & Yang Tan, T. T. (2008). Atomic layer deposition of TiO_2 nanostructures for self-cleaning applications. *Nanotechnology*, *19*(44), 445604. https://doi.org/10.1088/0957-4484/19/44/445604

Nikolaou, A., Meric, S., & Fatta, D. (2007). Occurrence patterns of pharmaceuticals in water and wastewater environments. *Analytical and Bioanalytical Chemistry*, *387*(4), 1225–1234. https://doi.org/10.1007/s00216-006-1035-8

Nishikawa, H., & Takahara, Y. (2001). Adsorption and photocatalytic decomposition of odor compounds containing sulfur using TiO_2/SiO_2 bead. *Journal of Molecular Catalysis A: Chemical*, *172*(1), 247–251. https://doi.org/10.1016/S1381-1169(01)00124-8

Ohko, Y., Iuchi, K., Niwa, C., Tatsuma, T., Nakashima, T., Iguchi, T., Kubota, Y., & Fujishima, A. (2002). 17β-estradiol degradation by TiO_2 photocatalysis as a means of reducing estrogenic activity. *Environmental Science & Technology*, *36*(19), 4175–4181. https://doi.org/10.1021/es011500a

Paschoalino, M. P., Kiwi, J., & Jardim, W. F. (2006). Gas-phase photocatalytic decontamination using polymer supported TiO_2. *Applied Catalysis B: Environmental*, *68*(1), 68–73. https://doi.org/10.1016/j.apcatb.2006.08.001

Pereira, L. C., de Souza, A. O., Bernardes, M. F. F., Pazin, M., Tasso, M. J., Pereira, P. H., & Dorta, D. J. (2015). A perspective on the potential risks of emerging contaminants to human and environmental health. *Environmental Science and Pollution Research*, *22*(18), 13800–13823. https://doi.org/10.1007/s11356-015-4896-6

Permpoon, S., Houmard, M., Riassetto, D., Rapenne, L., Berthomé, G., Baroux, B., Joud, J. C., & Langlet, M. (2008). Natural and persistent superhydrophilicity of SiO_2/TiO_2 and TiO_2/SiO_2 bi-layer films. *Thin Solid Films*, *516*(6), 957–966. https://doi.org/10.1016/j.tsf.2007.06.005

Rosenfeldt, E. J., & Linden, K. G. (2004). Degradation of endocrine disrupting chemicals bisphenol a, ethinyl estradiol, and estradiol during UV photolysis and advanced oxidation processes. *Environmental Science &*

Technology, *38*(20), 5476–5483. https://doi.org/10.1021/es035413p

Rusu, C. N., & Yates, J. T. (2001). N2O adsorption and photochemistry on high area TiO_2 powder. *The Journal of Physical Chemistry B*, *105*(13), 2596–2603. https://doi.org/10.1021/jp0040345

Singh, H. K., Saquib, M., Haque, M. M., Muneer, M., & Bahnemann, D. W. (2007). Titanium dioxide mediated photocatalysed degradation of phenoxyacetic acid and 2,4,5-trichlorophenoxyacetic acid, in aqueous suspensions. *Journal of Molecular Catalysis A: Chemical*, *264*(1), 66–72. https://doi.org/10.1016/j.molcata.2006.08.088

Sodré, F. F., Pescara, I. C., Montagner, C. C., & Jardim, W. F. (2010). Assessing selected estrogens and xenoestrogens in Brazilian surface waters by liquid chromatography-tandem mass spectrometry. *Microchemical Journal*, *96*(1), 92–98. https://doi.org/10.1016/j.microc.2010.02.012

Sodré, F. F., & Sampaio, T. R. (2020). Development and application of a SPE-LC-QTOF method for the quantification of micropollutants of emerging concern in drinking waters from the Brazilian capital. *Emerging Contaminants*, *6*, 72–81. https://doi.org/10.1016/j.emcon.2020.01.001

Takeda, S., Suzuki, S., Odaka, H., & Hosono, H. (2001). Photocatalytic TiO_2 thin film deposited onto glass by DC magnetron sputtering. *Thin Solid Films*, *392*(2), 338–344. https://doi.org/10.1016/S0040-6090(01)01054-9

Tolboom, S. N., Carrillo-Nieves, D., de Jesús Rostro-Alanis, M., de la Cruz Quiroz, R., Barceló, D., Iqbal, H. M. N., & Parra-Saldivar, R. (2019). Algal-based removal strategies for hazardous contaminants from the environment – A review. *Science of The Total Environment*, *665*, 358–366. https://doi.org/10.1016/j.scitotenv.2019.02.129

Trung, T., & Ha, C.-S. (2004). One-component solution system to prepare nanometric anatase TiO_2. *Materials Science and Engineering: C*, *24*(1), 19–22. https://doi.org/10.1016/j.msec.2003.09.004

Xu, L. P., Zhao, Y. X., Wu, Z. G., & Liu, D. S. (2003). A new method for preparing Ti-Si mixed oxides. *Chinese Chemical Letter*, *14*(11), 1159–1162. https://doi.org/http://www.qmtsg.com/qikan/726c45619f5c8c68ba3b61106b8ff674.html

Yu, H.-F., & Wang, S.-M. (2000). Effects of water content and pH on gel-derived TiO_2–SiO_2. *Journal of Non-Crystalline Solids*, *261*(1), 260–267. https://doi.org/10.1016/S0022-3093(99)00658-4

Zhang, Y., Zhou, J. L., & Ning, B. (2007). Photodegradation of estrone and 17β-estradiol in water. *Water Research*, *41*(1), 19–26. https://doi.org/10.1016/j.watres.2006.09.020